

Magnetoelastic contribution to the interface anisotropy of Pd/Co metallic multilayers

K. Kyuno, J.-G. Ha, and R. Yamamoto

Institute of Industrial Science, University of Tokyo, 7-22-1 Roppongi, Minato-ku, Tokyo 106, Japan

S. Asano

College of Arts and Sciences, University of Tokyo, 3-8-1 Komaba, Meguro-ku, Tokyo 153, Japan

(Received 31 July 1995; revised manuscript received 11 January 1996)

First-principles calculations of the magnetic anisotropy energies of Pd/Co metallic multilayers have been performed to investigate the effect of strain on the interface magnetic anisotropy. Also, to clarify the contribution of the interface to anisotropy, the anisotropy energies of an unsupported Co monolayer and bulk Co have been calculated. These two systems have different interfaces compared to the Pd/Co multilayer in the sense that an unsupported Co monolayer and bulk Co can be considered as vacuum/Co and Co/Co multilayers, respectively. A Pd/Co multilayer is predicted to exhibit a perpendicular magnetic anisotropy in accordance with experiment. Bulk Co shows perpendicular anisotropy, but the anisotropy energy is quite small compared to that of Pd/Co. On the contrary, an unsupported Co monolayer shows an in-plane anisotropy. These differences suggest the importance of the existence of the interface for perpendicular magnetic anisotropy, which originates from the modification of the local electronic structure of a Co layer due to the presence of the interface. The strength of the hybridization of electronic states at the interface determines the relative position of the Fermi energy to the position of the local density of states (LDOS) of $|m|=2$ character of Co d electrons of minority spin. If the LDOS of $|m|=2$ character is large at the Fermi energy, the system shows a perpendicular anisotropy. As for the effect of strain, the anisotropy energy of Pd/Co increases as a function of interatomic distance in the in-plane direction, while that of a Co monolayer decreases. Compared to these two systems, the magnetoelastic constant of bulk Co is considerably smaller. These results suggest that the effect of strain on the anisotropy energy is strongly correlated with the type of atomic species adjacent to the Co layer and cannot be determined solely from the value of strain introduced in the Co layer. In the case of a hetero-interface, the strength of hybridization between the orbitals inside the monolayer and that between the orbitals in adjacent monolayers are quite different and this fact leads to the large strain dependence of the anisotropy. [S0163-1829(96)02426-5]

I. INTRODUCTION

The realization of sophisticated techniques for ultrahigh vacuum deposition of magnetic materials has inspired many studies in recent years.¹⁻⁴ In particular, perpendicular magnetic anisotropy of metallic multilayers is currently of great interest in relation to high-density magnetic recording.⁵⁻⁷

There have been many experimental⁵⁻⁸ and theoretical⁹⁻¹² studies related to perpendicular magnetic anisotropy. It has been established phenomenologically that perpendicular anisotropy is associated with the interfaces between different metals, since the effective uniaxial anisotropy energy K_u can be expressed as a function of magnetic layer thickness t ,

$$K_u = K_v + 2K_s/t. \quad (1)$$

Here K_v and K_s represent a volume and interface contribution to magnetic anisotropy, respectively. K_v contains contributions from shape, magnetocrystalline, and magnetoelastic anisotropy, while K_s is interpreted as the interface anisotropy, which results from the broken symmetry of interface atoms, Néel's surface anisotropy.²²

There is currently a great deal of activity in attempts to understand the relationship between interfacial structures and the magnetic properties of ultrathin epitaxial layers. One important question relates to the role of elastic strain in influ-

encing magnetic anisotropy. Recently it has been pointed out by several authors that magnetoelastic energy, which is caused by the lattice mismatch strain at interface, is large enough to realize a perpendicular magnetic anisotropy.^{23,24}

A large lattice mismatch between adjacent layers leads to the formation of misfit dislocations at the interfaces, which reduce the coherency strains. Recently, Chappert and Bruno,²³ in a model of a single magnetic layer of thickness t on a rigid substrate, found that in the incoherent state residual misfit strains give rise to an anisotropy that is proportional to $1/t$. This implies that lattice misfit strain may contribute not only to the volume anisotropy (K_v) in coherent structures but also to the interface anisotropy (K_s) in incoherent structures, via the magnetoelastic effect. That is to say, the interface anisotropy consists of a Néel-type and a magnetoelastic anisotropy. Victoria and MacLaren^{16,17} also showed that strain was an important part of the interface anisotropy. It is to be noted that Néel interaction parameters can be expanded in a Taylor series as a function of strain and thus provide a magnetoelastic anisotropy. The term "Néel-type anisotropy," in the following, is taken to mean the magnetic anisotropy induced purely by the broken symmetry of the interface atoms.

Experimentally, however, the results for the contribution of the magnetoelastic anisotropy to surface anisotropy are rather controversial. Recently, Lee *et al.*⁸ explained the per-

pendicular magnetic anisotropy of Au/Co and Cu/Co multilayers in terms of strain-induced anisotropy without the use of Néel-type anisotropy. In addition, Nakamura *et al.*²⁵ also claimed that the perpendicular anisotropy of sputtered Pd/Co multilayers is caused mainly by interface strain anisotropy of interface alloys. On the other hand, Engel *et al.*²⁷ have synthesized Pd/Co multilayers with various crystal orientations and found that K_v could be fully accounted for by magnetoelastic and magnetocrystalline anisotropy contributions and that K_s was due only to Néel-type anisotropy. Awano *et al.*²⁸ have measured the magnetostriction constants of Cu/Co, Cu/Fe, Ag/Co, Pd/Co, and Au/Co multilayers. Their results suggest that the magnetic anisotropy cannot be explained only in terms of the stress-induced anisotropy. Since the atomic structures at the interfaces of metallic multilayers are not well known, the importance of the magnetoelastic contribution to the interface anisotropy is still unclear.

Therefore, to investigate the effect of elastic strain on interface magnetic anisotropy, we have performed a first-principles calculation of the magnetocrystalline anisotropy energies of Pd(2 ML)/Co(1 ML)(111) metallic multilayers. Also, to clarify the contribution of the interface to anisotropy, the anisotropy energies of an unsupported Co monolayer and bulk Co have been calculated. These two systems have different interfaces compared to Pd/Co multilayer in the sense that an unsupported Co monolayer and bulk Co can be considered as vacuum/Co and Co/Co multilayers, respectively.

II. METHOD OF CALCULATION

The calculation of the electronic structure has been done from first principles using the linear muffin-tin orbital method within the local spin-density approximation.²⁹ The magnetocrystalline anisotropy energy ΔE , which is the difference of the total energies for perpendicular ([001]) and in-plane ([100]) orientation of the magnetization, is given by the difference of sums over Kohn-Sham eigenvalues

$$\Delta E = \sum_{i,\mathbf{k}}^{\text{occ}} \varepsilon_i([\mathbf{100}], \mathbf{k}) - \sum_{i,\mathbf{k}}^{\text{occ}} \varepsilon_i([\mathbf{001}], \mathbf{k}). \quad (2)$$

Here $\varepsilon_i([\mathbf{001}], \mathbf{k})$ and $\varepsilon_i([\mathbf{100}], \mathbf{k})$ are the Kohn-Sham eigenvalues calculated with [001] and [100] spin polarization, respectively. Since the position of the Fermi level is an important factor, we evaluated the Fermi energy separately for different magnetization directions. The details of the calculation have been described in our previous papers.^{20,21}

The calculation has been done for three systems, i.e., the Pd/Co multilayer, the unsupported Co monolayer, and bulk Co. The model structure is illustrated schematically in Fig. 1. As mentioned earlier, the latter two systems have different interfaces compared to the Pd/Co multilayer in the sense that an unsupported Co monolayer and bulk Co can be considered as vacuum/Co and Co/Co multilayers, respectively. We will frequently denote the three systems as the X/Co multilayer ($X=\text{Pd}$, vacuum, and Co) in the following.

To analyze the results in terms of the different interfaces, the interatomic distance of Co in the in-plane direction (a) is assumed to take a common value for the three systems. In order to avoid extended computations the interface is as-

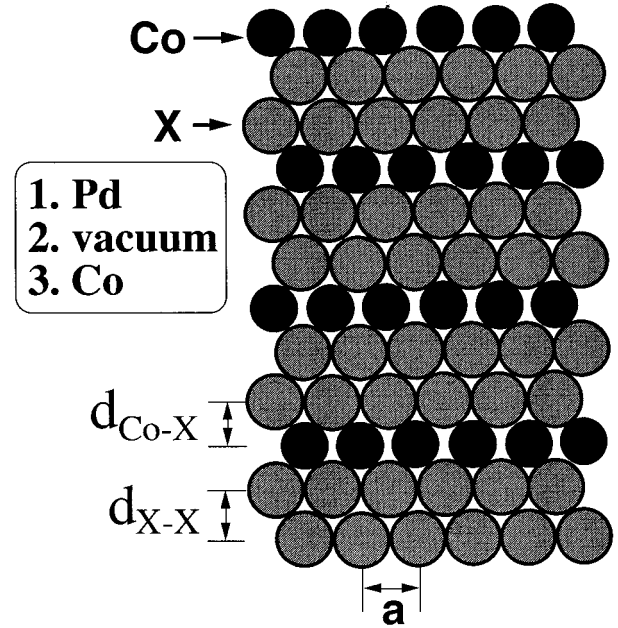


FIG. 1. Schematic illustration of the model structure adopted in the calculations.

sumed to be coherent. The interatomic distance of Co in the in-plane direction is taken to be equal to the bulk value of Pd. One period consists of two monolayers of X and one monolayer of Co. Each layer is a hexagonal plane and the atoms in the X layer are closely packed. The stacking sequence of these hexagonal planes is $ABCABC \dots$, like the close-packed planes of a face-centered-cubic structure.

The structure of an unsupported Co monolayer is equivalent to that of the Pd/Co multilayer, except that the atomic sphere of Pd is substituted by an empty sphere with the same radius. The effect of Pd on the magnetic anisotropy can be checked by the comparison of these two systems. The interplanar distances of X (d_{X-X}) of these two multilayers are equal to the bulk value of Pd. The interplanar distance of the interface between Co and X ($d_{\text{Co}-X}$) is the average of the bulk values of Co and Pd.

We have constructed the structure of bulk Co (the Co/Co multilayer) by expanding fcc Co isotropically in the close-packed plane so that the interatomic distance in the in-plane direction is equal to that of bulk Pd. The interplanar distance ($d_{X-X} = d_{\text{Co}-X}$) is contracted so as to keep the volume per atom equal to that of fcc Co. By considering the result of this system, we can clarify whether the interface region of the Co layer or the region far away from the interface is important for the perpendicular magnetic anisotropy in the case of a multilayer in which the Co layer thickness is more than 1 ML. This is because the electronic structure of bulk Co resembles the local electronic structure at the Co atom, which exists far away from the interface. The structure parameters (a , d_{X-X} , and $d_{\text{Co}-X}$) and atomic sphere radii (R_{Co} and R_X) adopted in the calculations are summarized in Table I.

As for the calculation of the elastic strain dependence of the anisotropy energy, the structure has been expanded in the in-plane direction isotropically. At the same time, the interplanar distance is contracted to keep the volume unchanged.

TABLE I. Structure parameters used in the calculations and results of the magnetocrystalline anisotropy energies.

System	a (Å)	$d_{\text{Co-X}}$ (Å)	$d_{\text{X-X}}$ (Å)	R_{Co} (Å)	R_{X} (Å)	ΔE (meV/unit cell)
Pd/Co	2.7505	2.1465	2.2458	1.4107	1.5480	1.12
Co monolayer	2.7505	2.1465	2.2458	1.4107	1.5480	-4.03
bulk Co	2.7505	1.6995	1.6995	1.3853	1.3853	0.13

III. RESULTS AND DISCUSSION

The results of the calculated anisotropy energies of X/Co ($X=\text{Pd}$, vacuum, and Co) multilayers are also shown in Table I. All the calculations are done with 9216 \mathbf{k} points in the whole Brillouin zone, which is sufficient to achieve a convergence better than 0.1 meV/unit cell. When ΔE is positive, the system shows a perpendicular anisotropy. Although the interatomic distances of Co in the in-plane direction are equal for the three systems, the calculated results are quite different. As in the previous calculations,²⁰ Pd/Co shows a perpendicular anisotropy in accordance with experiments. By using the experimental K_v value,²⁷ K_s can be calculated as 1.42 ergs/cm². This is somewhat larger compared to the experimental values 0.92 and 0.63 erg/cm² by den Broeder *et al.*⁶ and Engel *et al.*,²⁷ respectively. Engel *et al.*²⁷ found that the in-plane Co lattice constant is quite close to a compositional average of the Co and Pd lattice constants that is smaller than the lattice constant we assumed in our hypothetical model. As will be shown later, the anisotropy energy of the Pd/Co multilayer increases as a function of in-plane lattice constants and the difference in structure could be the origin of the discrepancy. As for bulk Co, the calculated anisotropy energy is positive, but the absolute value is smaller than that of the Pd/Co multilayer. On the contrary, an unsupported Co monolayer exhibits an in-plane anisotropy. The absolute value of the anisotropy energy is more than three times larger than that of the Pd/Co multilayer.

From these results, it can be concluded that the effect of the interface between X and Co on the magnetic anisotropy, i.e., interface anisotropy, depends strongly on the type of X layer adjacent to the Co layer. The small anisotropy energy

of bulk Co suggests that in the case of a multilayer in which the Co layer thickness is more than 1 ML, the contribution of the Co atoms far away from the interface to the perpendicular anisotropy will be small even if the Co layer is stretched in the in-plane direction. Therefore the interface between different metals is necessary to realize a large perpendicular anisotropy.

To find the origin of the interface anisotropy and to understand the reason why the anisotropy energy differs so much as to X , we analyzed the electronic structure of the three systems. The magnetic anisotropy originates from the spin-orbit interaction, which couples eigenstates ψ_{nk} and $\psi_{n'k}$ with eigenvalues ϵ_{nk} below the Fermi energy (ϵ_F) and $\epsilon_{n'k}$ above ϵ_F . Here $n(n')$ and k label the energy band and a point in the Brillouin zone, respectively. If the level splitting $\epsilon_{nk} - \epsilon_{n'k}$ is much larger than the spin-orbit coupling parameter ξ , perturbation theory can be used to calculate the anisotropy energy. The corrections to the energy level ϵ_{nk} due to the spin-orbit coupling are given as

$$\Delta \epsilon_{nk} = \sum_{\epsilon_{n'k} > \epsilon_F}^{n'} \frac{|\langle \psi_{nk} | H_{\text{s.o.}}(\theta, \varphi) | \psi_{n'k} \rangle|^2}{\epsilon_{nk} - \epsilon_{n'k}}. \quad (3)$$

The expression is given within the lowest order, i.e., second order, because the diagonal matrix elements of $H_{\text{s.o.}}(\theta, \varphi)$ are zero. Here $H_{\text{s.o.}}(\theta, \varphi)$ is a spin-orbit coupling matrix ξl_s and the magnetization is oriented along the (θ, φ) . θ and φ are polar coordinates with respect to a rectangular coordinate system. The z axis of the coordinate system is chosen normal to the film plane and the x axis is chosen along a nearest-neighbor direction.

From Eq. (3) the magnetic anisotropy can be expressed as

$$\Delta E = \sum_k \sum_{\epsilon_{nk} < \epsilon_F}^n \sum_{\epsilon_{n'k} > \epsilon_F}^{n'} \frac{\{|\langle \psi_{nk} | H_{\text{s.o.}}(\pi/2, 0) | \psi_{n'k} \rangle|^2 - |\langle \psi_{nk} | H_{\text{s.o.}}(0, 0) | \psi_{n'k} \rangle|^2\}}{\epsilon_{nk} - \epsilon_{n'k}}. \quad (4)$$

The negative and positive values of the element $\{|\langle \psi_{nk} | H_{\text{s.o.}}(\pi/2, 0) | \psi_{n'k} \rangle|^2 - |\langle \psi_{nk} | H_{\text{s.o.}}(0, 0) | \psi_{n'k} \rangle|^2\}$ contribute to perpendicular and in-plane anisotropy, respectively. The explicit form of the spin-orbit matrix elements between d orbitals as a function of magnetization direction θ and φ are explained in detail by Takayama, Bohnen, and Fulde.³¹ As for the interaction between the orbitals of the same spin, the matrix elements $\langle d_{xz} | H_{\text{s.o.}} | d_{yz} \rangle$ and $\langle d_{xy} | H_{\text{s.o.}} | d_{x^2-y^2} \rangle$ contribute to perpendicular anisotropy and $\langle d_{x^2-y^2} | H_{\text{s.o.}} | d_{yz} \rangle$, $\langle d_{xy} | H_{\text{s.o.}} | d_{xz} \rangle$, and $\langle d_{3z^2-r^2} | H_{\text{s.o.}} | d_{yz} \rangle$ contribute to in-plane anisotropy. The relative value of these elements are $\langle d_{xz} | H_{\text{s.o.}} | d_{yz} \rangle : \langle d_{xy} | H_{\text{s.o.}} | d_{x^2-y^2} \rangle : \langle d_{x^2-y^2} | H_{\text{s.o.}} | d_{yz} \rangle : \langle d_{xy} | H_{\text{s.o.}} | d_{xz} \rangle : \langle d_{3z^2-r^2} | H_{\text{s.o.}} | d_{yz} \rangle = -1 : -4 : 1 : 1 : 3$. These matrix elements exist only between eigenstates at the same k point. However, since the absolute value of the matrix element $\langle d_{xy} | H_{\text{s.o.}} | d_{x^2-y^2} \rangle$ is the largest, and this element contributes to perpendicular anisotropy by the lifting of the degeneracy at high-symmetry points in the Brillouin zone, the origin of the perpendicular anisotropy can be discussed qualitatively from the relative position of the Fermi level to the local density of states (LDOS) of $|m|=2$ character of Co minority spin d electrons.

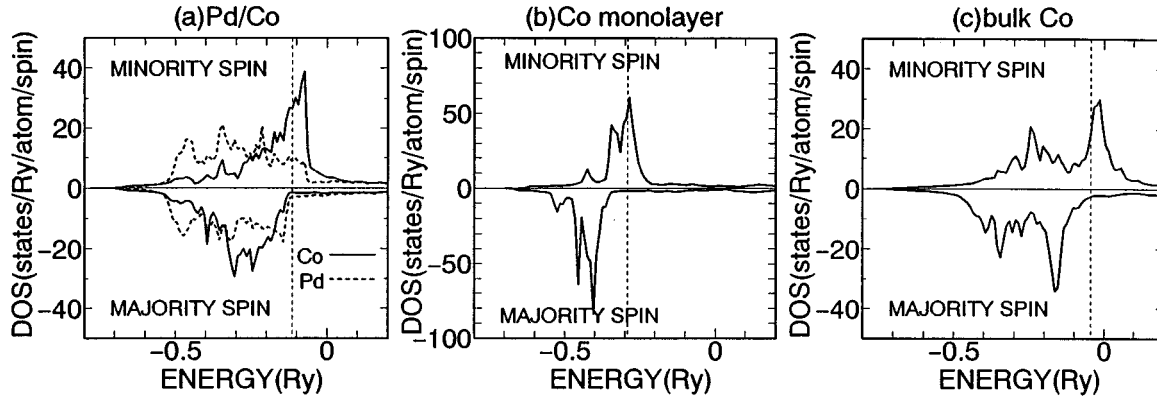


FIG. 2. Local density of states (LDOS) for the three systems. The vertical broken lines represent Fermi energies. (a) Pd/Co multilayer (solid line, LDOS of Co, broken line, LDOS of Pd), (b) Co monolayer, and (c) bulk Co.

Figure 2 shows the (LDOS) of the three systems. The majority spin band is almost filled in all systems. The width of the LDOS of Co becomes larger on the order Co monolayer, Pd/Co multilayer, and bulk Co. The LDOS of Co in the Co monolayer is very narrow because the coordination number of Co atom is smaller than in the case of the Pd/Co multilayer or bulk Co. The hybridization of the orbitals is almost restricted inside the atomic plane of Co. The width of the LDOS of Co in the Pd/Co multilayer is larger than that of the Co monolayer, but smaller than that of bulk Co. This is a consequence of the fact that the orbitals of Co can hybridize with the orbitals of Pd, as can be seen from Fig. 2, but the hybridization is smaller than in the case of bulk Co.

Figure 3(a) shows the magnetic anisotropy energy of Pd/Co as a function of band filling. Band filling is the number of valence electrons per unit cell. The anisotropy energy shows an oscillatory behavior. The peak near the Fermi level causes perpendicular anisotropy. This peak near the Fermi level is characteristic in the sense that it appears also in the cases of Pt/Co, Cu/Co, Ag/Co, and Au/Co multilayers.²⁰ Figure 4(a) shows the m -decomposed LDOS of Co. The LDOS is plotted as a function of band filling to see the correspondence to Fig. 3 easily. The increase of the magnetic anisotropy from a band filling of about 25–29 can be attributed to the large LDOS of $|m|=2$ character of minority spin below

the Fermi level. This is the origin of the characteristic peak of ΔE as a function of band filling near the Fermi-level.

The dependence of the anisotropy energy on the band filling of a Co monolayer is shown in Fig 3(b). There is a very sharp negative peak near the Fermi level and a Co monolayer exhibits a strong in-plane anisotropy. This sharp peak corresponds to the large LDOS of the $d_{3z^2-r^2}$ orbital near the Fermi level [Fig. 4(b)]. This results from the small hybridization of the $d_{3z^2-r^2}$ orbital with other orbitals because this orbital extends perpendicularly to the film plane into the vacuum region. The $d_{3z^2-r^2}$ orbital contributes to in-plane anisotropy because of the matrix element $\langle d_{3z^2-r^2} | H_{s.o.} | d_{yz} \rangle$.

The results for bulk Co are shown in Fig. 3(c). Although there is a positive peak near the band filling of about 29, just as in the case of Pd/Co, the Fermi level comes right at the crossover from in-plane to perpendicular anisotropy and this system exhibits a small perpendicular anisotropy. The peak above the Fermi level originates from the fact that the LDOS of the d_{xy} and $d_{x^2-y^2}$ orbitals is large just above the Fermi level [Fig. 4(c)].

From these results the difference of the anisotropy of these three systems can be explained systematically. In Fig. 5 the LDOS of the Co minority spin is illustrated schemati-

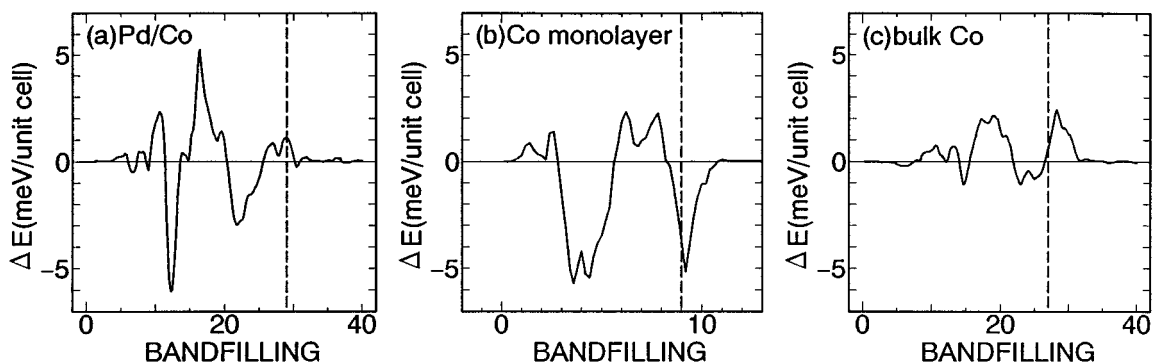


FIG. 3. Magnetic anisotropy energy as a function of band filling. The vertical broken lines represent Fermi levels that correspond to 29, 9, and 27 valence electrons per unit cell for the (a) Pd/Co multilayer, (b) Co monolayer, and (c) bulk Co, respectively.

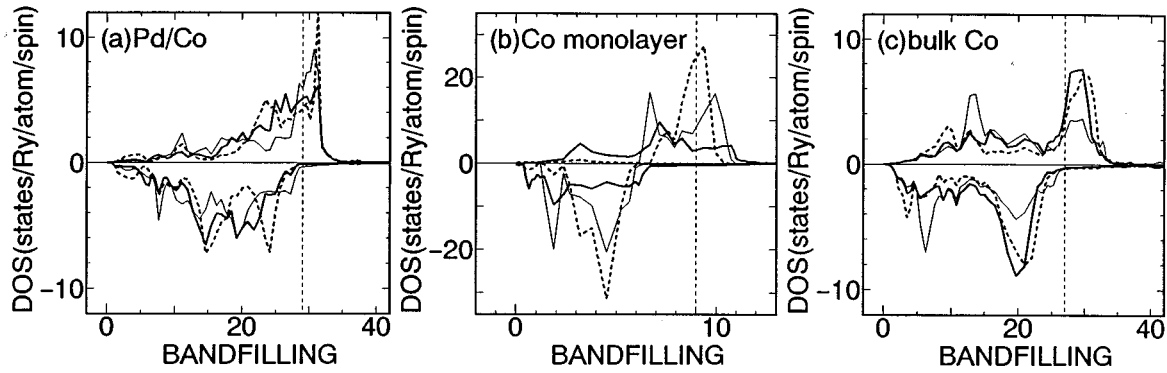


FIG. 4. m -decomposed LDOS of Co. The vertical broken lines represent Fermi levels. (a) Co in the Pd/Co multilayer, (b) the Co monolayer, and (c) bulk Co. Thick solid, thin solid, and dotted lines correspond to $d_{x^2-y^2}(d_{xy})$, $d_{xz}(d_{yz})$, and $d_{3z^2-r^2}$ orbitals, respectively.

cally. As for the bulk Co, the LDOS is divided into the bonding and antibonding states. In the case of Pd/Co the Fermi level moves closer to the peak above the Fermi level compared to the case of bulk Co. This is caused by the depression of the LDOS in the lower-energy region, which originates from the reduced hybridization at the interface. In the case of a Co monolayer the Fermi energy moves much closer to the peak. This also originates from the depression of the LDOS in the lower-energy region because there are no orbitals to hybridize with in the vacuum region.

In Fig. 6 the relation between the m -decomposed LDOS of Co minority spin [Fig. 6(a)] and the anisotropy energy near the Fermi energy [Fig. 6(b)] is schematically illustrated. The position of the Fermi energy changes according to the strength of hybridization at the interface as shown in Fig. 5. If the LDOS of $|m|=2$ character, d_{xy} and $d_{x^2-y^2}$ orbitals, is large at the Fermi energy, the system shows perpendicular anisotropy. In the case of Pd/Co, since the LDOS of $|m|=2$ character is large at the Fermi level, this system exhibits perpendicular anisotropy. By substituting the Pd layer by a Co layer, the hybridization at the interface is enhanced,

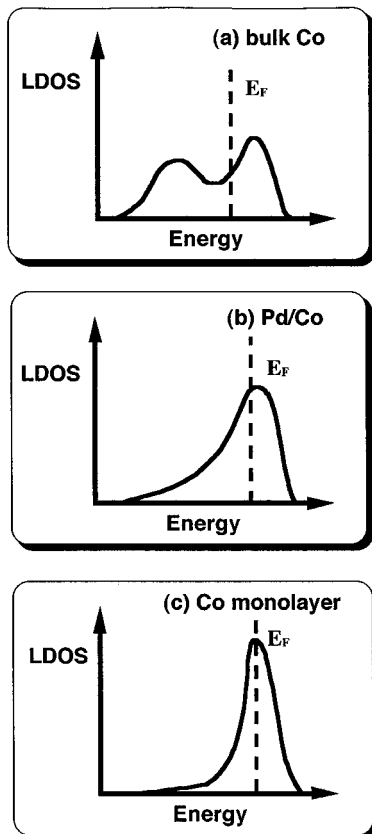


FIG. 5. Schematic illustration of the LDOS of Co minority spin for the three systems.

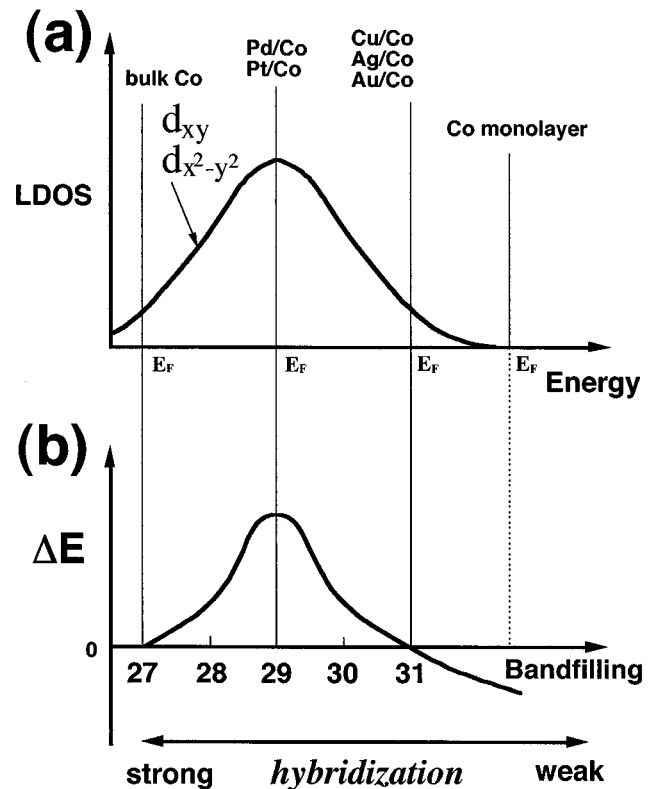


FIG. 6. Schematic illustration of (a) the LDOS of $|m|=2$ character of Co minority spin near the Fermi level and (b) the dependence of anisotropy energy as a function of band filling and strength of hybridization.

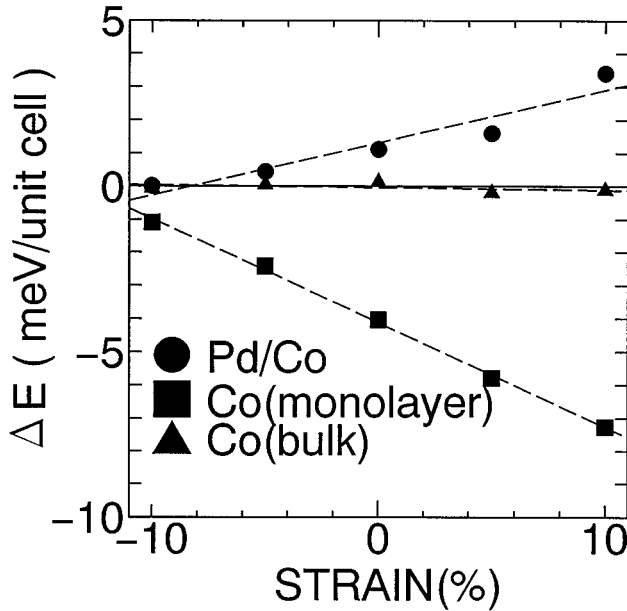


FIG. 7. Strain dependence of the magnetocrystalline anisotropy energy. Dashed curves are the least-squares fit.

which leads to the position change of the Fermi level and hence to the decrease of anisotropy energy. On the other hand, if the Pd layer is substituted by a vacuum layer, the hybridization at the interface is reduced and the anisotropy energy becomes smaller. In this way, the anisotropy can be explained in terms of the strength of hybridization at the interface.

In previous studies we have plotted ΔE of Pt/Co, Cu/Co, Ag/Co, and Au/Co as a function of band filling and showed that there is a characteristic peak near the Fermi level also for these systems.²⁰ The peak is just the one illustrated in Fig. 6(b) and those systems previously studied are also plotted at the corresponding band fillings. The hybridization at the interface of Cu/Co, Ag/Co, and Au/Co multilayers is smaller than that of Pd/Co because the energy levels of the d electrons of Cu, Ag, and Au are deeper than that of Pd. As a consequence, the Fermi level is located on the right-hand side of the peak in the ΔE -band filling plot. A Co monolayer

can be thought of as the limit of weak hybridization at the interface. It can be concluded that the perpendicular anisotropy originates from the hybridization at the interface.

The anisotropy energies of the three systems are shown in Fig. 7 as a function of elastic strain in the in-plane direction. There are a few noticeable features, which can be seen in Fig. 7. The first one is that the dependence of anisotropy energy on strain is opposite for a Pd/Co multilayer and a Co monolayer. Although the anisotropy energy of the Pd/Co multilayer increases as a function of strain, that of a Co monolayer decreases. This fact suggests that the effect of strain on the anisotropy energy is strongly correlated with the type of atomic species adjacent to the Co layer and cannot be determined solely from the value of strain introduced in the Co layer.

The second feature is the strong strain dependence of the anisotropy energy of Pd/Co and Co monolayers in contrast to the weak strain dependence of bulk Co. By the least-squares fit of the anisotropy energies as a function of strain, we have evaluated the magnetostriction constants. The magnetostriction constant is calculated assuming $K_u = -\frac{3}{2}\lambda\sigma$ for strain-induced magnetoelastic energy,²⁴ with the biaxial elastic modulus of bulk Co, 4.1×10^{11} N/m². λ and σ are the magnetostriction constant and stress, respectively. The calculated value of the magnetostriction constants are -3.1×10^{-4} , 6.1×10^{-4} , and 1.4×10^{-5} for the Pd/Co multilayer, the Co monolayer, and bulk Co, respectively. The value for Pd/Co is more than one order larger than that for bulk Co. Recently, Takahashi *et al.*²⁶ have investigated the magnetostriction constants of a PdCo alloy and a Pd/Co multilayer by measuring the magnetic anisotropy energy induced by the application of in-plane uniaxial strain. As in our calculations, the magnetostriction constant of the Pd/Co multilayer is much larger than that of bulk Co. The magnetostriction constants of fcc Co was obtained to be 0.2×10^{-4} from the extrapolation of the data of alloy films, while the value of Pd/Co multilayers with a Co layer thickness of 2.5 Å was 0.9×10^{-4} . The magnetostriction constant of Pd/Co measured by Hashimoto, Ochiai, and Aso³⁰ is -1.5×10^{-4} , which is closer to the theoretical value.

To find the origin of the strain dependence of the anisotropy energy, we calculated the anisotropy for various band fillings. The result for Pd/Co is shown in Fig. 8(a) for each

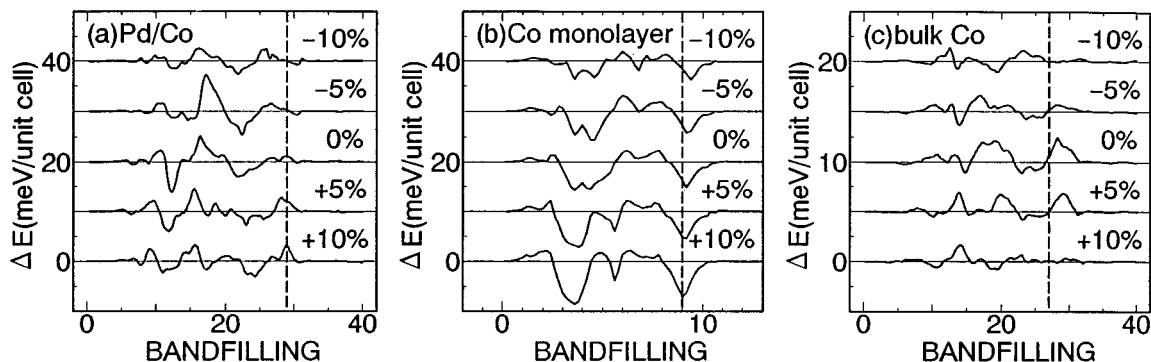


FIG. 8. Anisotropy energy as a function of band filling. The vertical lines represent Fermi levels. (a) Pd/Co multilayer, (b) Co monolayer, and (c) bulk Co. Values of strain in the in-plane direction are indicated.

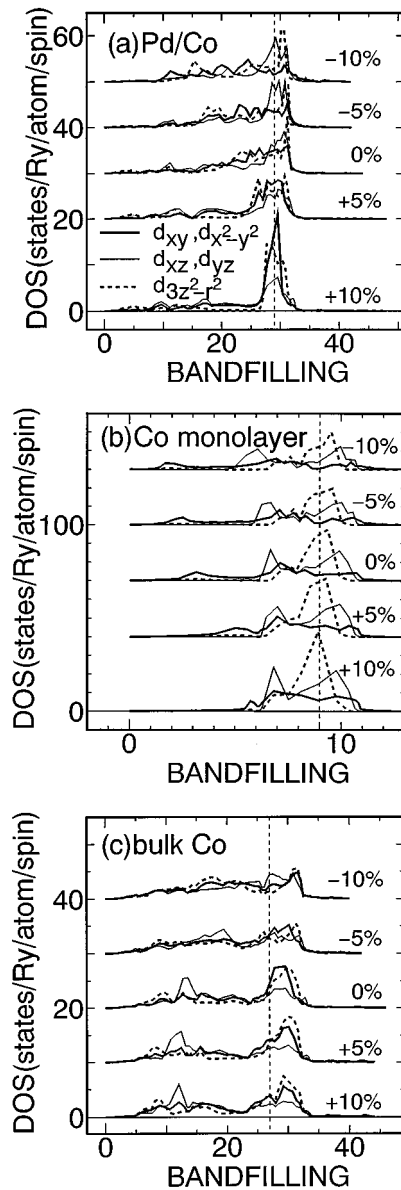


FIG. 9. m -decomposed LDOS of the minority spin of Co. The vertical broken lines represent Fermi levels. (a) Co in the Pd/Co multilayer, (b) the Co monolayer, and (c) bulk Co. Thick solid, thin solid, and dotted lines correspond to $d_{x^2-y^2}$ (d_{xy}), d_{xz} (d_{yz}), and $d_{3z^2-r^2}$ orbitals, respectively. Values of strain in the in-plane direction are indicated.

strain. We can see that the broad peak near the Fermi level approaches the Fermi level as the strain increases and the increase of anisotropy energy results. In Fig. 9(a) the m -decomposed LDOS of Co minority spin is shown as a function of band filling. As the value of strain increases, the hybridization in the in-plane direction becomes weaker and consequently the width of the LDOS becomes smaller. At the same time, the region where the LDOS of d_{xy} and $d_{x^2-y^2}$ orbitals is large, which corresponds to a band filling of about 20–25 in the -10% case, moves towards the Fermi level. This is strongly correlated with the movement of the peak of ΔE in Fig. 8(a).

The results for the Co monolayer are shown in Figs. 8(b) and 9(b). The negative peak near the Fermi level in Fig. 8(b) becomes larger as a function of strain. This corresponds to

the increase of the LDOS of the $d_{3z^2-r^2}$ orbital near the Fermi level as a function of strain shown in Fig. 9(b). This tendency is caused by the reduced hybridization of the $d_{3z^2-r^2}$ orbital with other orbitals as the interatomic distance in the plane direction increases.

The results for bulk Co are shown in Figs. 8(c) and 9(c). The anisotropy energy is nearly constant at zero near the Fermi level in the case of -10% and $+10\%$ strain. For the -5% , 0% , and $+5\%$ systems, the Fermi level comes near the position where the anisotropy energy changes from a negative to a positive value. The relative position of the Fermi level to the LDOS of $|m|=0, 1$, and 2 character does not change as drastically as a function of strain as in other two systems and this fact leads to the small strain dependence of anisotropy energy. By increasing the strain, which accompanies the contraction of interplanar distance, the hybridization between the orbitals in the in-plane direction becomes smaller. But in the case of bulk Co, the species in the adjacent layers are also Co. Therefore the reduced hybridization in the in-plane direction can be compensated by the increase in hybridization between the orbitals in adjacent monolayers. This is the origin of the small changes of the relative position of the Fermi level to the LDOS of $|m|=0, 1$, and 2 character. This is in contrast to systems where the atomic species in adjacent monolayers are different. In the case of a heterointerface, the strength of hybridization between the orbitals inside the monolayer and that between the orbitals in adjacent layers are quite different and this fact leads to large strain dependence of anisotropy.

IV. CONCLUSION

In summary, we have calculated the magnetocrystalline anisotropy energies of the three systems X/Co ($X=\text{Pd}$, vacuum, and Co) to investigate the origin of the interface anisotropy and effect of elastic strain. The calculated results are dramatically different for these three systems. The Pd/Co multilayer shows a perpendicular magnetic anisotropy that is in good agreement with experiments. Bulk Co also exhibits a perpendicular anisotropy, but the anisotropy energy is about one order smaller than that of a Pd/Co multilayer. On the contrary, a Co monolayer shows a very large in-plane anisotropy. It is concluded that the interface anisotropy originates by the electronic hybridization at the interface.

As for the effect of strain, the anisotropy energy of Pd/Co increases as a function of interatomic distance in the in-plane direction, while that of a Co monolayer decreases. Compared to these two systems, the magnetoelastic constant of bulk Co is considerably smaller. These results suggest that the effect of strain on the anisotropy energy is strongly correlated with the type of atomic species adjacent to the Co layer and cannot be determined solely from the value of strain introduced in the Co layer. In the case of a heterointerface, the strength of hybridization between the orbitals inside the monolayer and that between the orbitals in adjacent layers are quite different and this fact leads to the large strain dependence of the anisotropy.

ACKNOWLEDGMENT

This work was supported by a Grant-in-Aid for Scientific Research from the Ministry of Education, Science, Sports and Culture, Japan, No. 06452325.

- ¹*Thin Film Growth Techniques for Low-Dimensional Structures*, edited by R. F. C. Farrow, S. S. P. Parkin, P. J. Dobson, J. H. Neave, and A. S. Arrot (Plenum, New York, 1987).
- ²*Growth, Characterization, and Properties of Ultrathin Magnetic Films and Multilayers*, edited by B. Jonker, J. P. Heremans, and E. E. Marinero, MRS Symposia Proceedings No. 151 (Materials Research Society, Pittsburgh, 1989).
- ³I. K. Schuller, in *Physics, Fabrication and Applications of Multilayered Structures*, edited by P. Dhez and C. Weisbuch (Plenum, New York, 1988), p. 139.
- ⁴B. Heinrich and J. F. Cochran, *Adv. Phys.* **42**, 523 (1993).
- ⁵P. F. Carcia, and A. D. Meinhaldt, and A. Suna, *Appl. Phys. Lett.* **47**, 178 (1985).
- ⁶F. J. A. den Broeder, D. Kuiper, H. C. Donkersloot, and W. Hoving, *Appl. Phys. A* **49**, 507 (1989).
- ⁷F. J. A. den Broeder, D. Kuiper, A. P. van de Mosselaer, and W. Hoving, *Phys. Rev. Lett.* **60**, 2769 (1988).
- ⁸C. H. Lee, Hui He, F. J. Lamelas, W. Vavra, C. Uher, and R. Clarke, *Phys. Rev. B* **42**, 1066 (1990).
- ⁹W. Karas, J. Noffke, and L. Fritsche, *J. Chim. Phys. Phys. Chim. Biol.* **86**, 861 (1989).
- ¹⁰C. Li, A. J. Freeman, and C. L. Fu, *J. Magn. Magn. Mater.* **83**, 51 (1990).
- ¹¹J. G. Gay and R. Richter, *Phys. Rev. Lett.* **56**, 2728 (1986).
- ¹²G. H. O. Daalderop, P. J. Kelly, and M. F. H. Schuurmans, *Phys. Rev. B* **42**, 7270 (1990).
- ¹³R. Wu, C. Li, and A. J. Freeman, *J. Magn. Magn. Mater.* **99**, 71 (1991).
- ¹⁴S. Pick, J. Dorantes-Dávila, G. M. Pastor, and H. Dreyssé, *Phys. Rev. B* **50**, 993 (1994).
- ¹⁵J. M. MacLaren and R. H. Victora, *J. Appl. Phys.* **76**, 6069 (1994).
- ¹⁶R. H. Victora and J. M. MacLaren, *J. Appl. Phys.* **73**, 6415 (1993).
- ¹⁷R. H. Victora and J. M. MacLaren, *Phys. Rev. B* **47**, 11 583 (1993).
- ¹⁸P. Bruno, *J. Phys. F* **18**, 1291 (1988).
- ¹⁹P. Bruno and J.-P. Renard, *Appl. Phys. A* **49**, 499 (1989).
- ²⁰K. Kyuno, R. Yamamoto, and S. Asano, *J. Phys. Soc. Jpn.* **61**, 2099 (1992).
- ²¹K. Kyuno, R. Yamamoto, and S. Asano, *Model. Simul. Mater. Sci. Eng.* **1**, 133 (1993).
- ²²L. Néel, *J. Phys. Radium* **15**, 225 (1954).
- ²³C. Chappert and P. Bruno, *J. Appl. Phys.* **64**, 5736 (1988).
- ²⁴A. Yamaguchi, S. Ogu, W.-H. Soe, and R. Yamamoto, *Appl. Phys. Lett.* **62**, 1020 (1993).
- ²⁵K. Nakamura, S. Tsunashima, M. Hasegawa, and S. Uchiyama, *J. Magn. Magn. Mater.* **93**, 462 (1991).
- ²⁶H. Takahashi, S. Tsunashima, S. Iwata, and S. Uchiyama, *Jpn. J. Appl. Phys.* **32**, L1328 (1993).
- ²⁷B. N. Engel, C. D. England, R. A. van Leeuwen, M. H. Wiedmann, and C. M. Falco, *J. Appl. Phys.* **70**, 5873 (1991).
- ²⁸H. Awano, O. Taniguchi, T. Katayama, F. Inoue, A. Itoh, and K. Kawanishi, *J. Appl. Phys.* **64**, 6107 (1988).
- ²⁹O. K. Andersen, *Phys. Rev. B* **12**, 3060 (1975).
- ³⁰S. Hashimoto, Y. Ochiai, and K. Aso, *J. Appl. Phys.* **66**, 4909 (1989).
- ³¹H. Takayama, K.-P. Bohnen, and P. Fulde, *Phys. Rev. B* **14**, 2287 (1976).